Intermolecular Interactions in Crystalline Hydrates – What Can a Crystallographer Learn from Theoretical Calculations?*

Kersti Hermansson

Department of Chemistry, Uppsala University, Box 531, S-751 21 Uppsala, Sweden

Hermansson, K., 1987. Intermolecular Interactions in Crystalline Hydrates – What Can a Crystallographer Learn from Theoretical Calculations? – Acta Chem. Scand., Ser. A 41: 513–526.

Energies and electron distributions in crystalline hydrates, and the way in which they are affected by various components in the crystalline environment are examined. Non-additive effects are in general found to give an appreciable contribution to interaction energies, but not to the electron rearrangement. Qualitative and quantitative features of the electron redistribution are discussed. The overall agreement between experimental and theoretical densities is found to be satisfactory for high quality studies, but the magnitude of the intermolecular effects is at the limit of what can be measured experimentally today.

The molecular properties commonly derived in a diffraction analysis of a crystal, i.e. bond distances, anisotropic atomic displacement parameters and, from X-ray studies, electron distributions, are all probes of the structural environment. The picture is complicated, however, by the fact that these quantities are averages over all modes of vibration in a crystal, over all crystallographic unit cells, and over time.

Although "standard" diffraction refinements in some cases yield biased *positional parameters* which are in error by several hundredths of an Ångström (even when the precision is of the order of 0.001 Å), it is fair to say that diffraction is an unsurpassed technique for obtaining accurate molecular geometries in a crystal. Dynamical processes in the crystal are much more complex, however, and the atomic displacement parameters (*"thermal ellipsoids"*) obtained by diffraction give a very limited picture because of vibrational averaging. Other experimental techniques available, in particular inelastic neutron scattering and IR and Raman spectroscopy, provide much valuable information about internal and external vibrations in molecular crystals, but both have their limitations. Within the restriction of using a classical theory of motion and a simplified interaction model, Molecular Dynamics and Lattice Dynamics provide means of studying directly the dynamics of many-body systems at the molecular level (see, for example, Ref. 1). The interpretation of the experimental data could, in many cases, benefit greatly from the availability of results from such calculations.

Finally, *the electron density* is, in principle, the quantity most readily available from X-ray diffraction studies. However, the total molecular electron density is heavily dominated by the constituent atomic densities, and the electron redistribution due to intra- and especially intermolecular bonding is comparatively small. Consequently, bonding features in experimental electron density maps are easily affected by random and systematic experimental errors and errors in (or the inappropriateness of) the refined model (for a thorough account of errors in experimental electron density maps, see, for example, Rees[2] and Feil[3]). As a rule-of-thumb, the accuracy of experimental density maps is at best 0.05 e $Å^{-3}$. Quantum-mechanically derived electron densities could here be a useful complement to experiment and provide an independent measure of the effects of intermolecular electron rear-

*Presented at the *XII Nordiska Strukturkemistmötet* in Sånga-Säby, Sweden, June 8–13, 1987.

rangements. However, model calculations can also provide quantities not directly obtainable from diffraction experiments, such as energies, and, unlike experiment, provide the possibility of studying contributions from different components in the environment separately.

In view of the complexity of condensed phase systems, it is clear that it is desirable, whenever possible, to perform different kinds of model calculations on one and the same system in order to gain a more complete understanding of its chemistry and physics. Some appropriate techniques applicable to the study of a molecular crystal are: (1) quantum-mechanical calculations (electron density, energies, forces, ...), (ii) energy minimization techniques, (iii) Lattice Dynamics calculations, and (iv) Molecular Dynamics simulations. The last three methods are discussed in some detail in Ref. 4 in connection with their application to the $LiHCOO \cdot H_2O$ crystal and will be discussed only very briefly in the present paper. Here, we focus on electron densities and interaction energies obtained from *ab initio* calculations. The first section of the review describes the computational details, while the second section tries to answer the question "can X-ray diffraction detect intermolecular bonding effects?" by discussing the magnitudes and characteristic features of experimental and theoretical electron rearrangements for the water molecule in various external fields.

Crystallographers discuss chemical bonding mainly in terms of bond distances and electron densities, while other chemists and physicists focus on interaction energies. However, the understanding of chemical bonding greatly profits from a *simultaneous* discussion of interaction energies and electron density redistributions. This point is emphasized in the third section of the paper, where non-additive contributions to interaction energies and electron densities are discussed.

The examples given in this review are all concerned with the water molecule in crystalline hydrates or small aqua complexes. There are many reasons for this choice: (i) The bonding in aqueous systems is of prime importance in chemistry and physics. (ii) In the systems discussed here, the water molecule participates in hydrogen bonding, cation-water bonding and anion-water bonding; the systems thus represent a logical sequence for comparison of the effects of different types of intermolecular bonding on one and the same molecule. (iii) Small aqua complexes lend themselves readily to extended quantum-mechanical calculations. (iv) Water is the molecule for which there is most experimental data – not least from neutron and X-ray diffraction. (v) Many of the conclusions drawn from the hydrate studies can be useful in the discussion of intermolecular interactions in other molecular crystals.

Numerous reviews on intermolecular interactions and electron density distributions exist; see e.g. Pullman,[6] Raznakievich and Orville-Thomas,[6] Hirshfeld,[7] and Coppens and Hall.[8]

Electron density distributions – can we see evidence of intermolecular interactions using X-rays?

Derivation of electron densities and interaction energies. Two types of *difference* or *deformation electron densities* are discussed. In the first type, the reference density consists of a superposition of free, spherical, or spherically averaged atoms or atomic ions, i.e.:

$$\Delta\varrho(r) = \varrho^{\mathrm{tot}}(r) - \sum_{\text{atom } i} \varrho_i(r). \qquad (1)$$

The deformation density in (1) includes the effects of both the intra- and intermolecular bonding, the former generally being the far more dominant feature. The intermolecular bonding is more clearly exposed by using a reference density of superposed free undistorted molecules or ions, i.e.:

$$\Delta\varrho(r) = \varrho^{\mathrm{tot}}(r) - \sum_{\substack{\text{mole-}\\ \text{cule } i}} \varrho_i(r), \qquad (2)$$

where "molecule" means any constituent building block (molecule or ion). The atomic arrangement in (1) and the reference molecules in (2) have the same geometry as in the bonded complex. The consequences of using this same geometry have been discussed by Hermansson.[9]

Experimental difference density maps obtained by diffraction are almost exclusively of type (1). Here, the total density is calculated from a Fourier summation over the observed X-ray structure factors. The reference density is obtained from calculated structure factors based on conven-

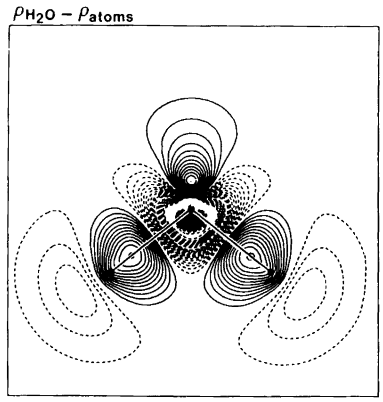

a

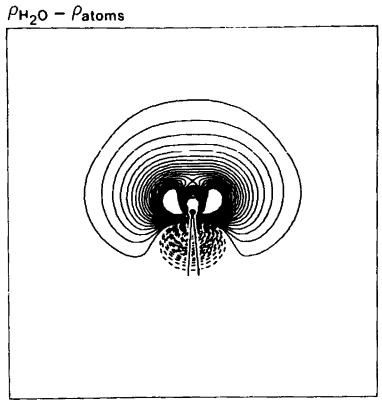

b

Fig. 1. Deformation electron density [of type (1)] for a free water molecule (a) in the molecular plane and (b) bisecting the H–O–H angle. Basis sets used were Dunning's[16] <5*s*3*p*/3*s*> contraction of Huzinaga's[17] (10*s*6*p*/5*s*) basis for O/H with polarization functions according to Roos and Siegbahn.[18] Positive contours (electron excess) are drawn as solid lines, negative contours (electron deficiency) are dashed; the zero contour is omitted. Contour levels at ±0.05, ±0,10,... e Å^{-3}.

tional spherical-atom scattering factors but using positional and thermal parameters which are hopefully closer to the true nuclear parameters than those derived from a conventional spherical-atom X-ray least-squares refinement. In the *X–N technique,*[10] these calculated structure factors are based on positional and thermal parameters determined by neutron diffraction. In the *X–X$_{high}$ technique,* the atomic parameters of the reference state are derived from a least-squares refinement using only high-order X-ray data, where the contribution from the valence electrons to the total scattering is small. Another approach to the derivation of experimental deformation density maps is to use non-spherical scattering factors in an X-ray *multipolar deformation refinement* (see, for example, Stewart[11] and Hirshfeld[12]).

Possible sources of error in experimentally derived electron densities were mentioned briefly in the introductory section. It is also well known that electron distributions and energies derived from *ab initio* calculations within the Hartree-Fock framework are by no means void of error. Basis-set effects and correlation effects are two of the most important sources of error for light-atom systems. The literature on the subject is vast. A recent review on the errors in theoretical electron density maps is given by Breitenstein *et al.*;[13] see also Smith[14] and Feil.[15]

Small water-ion clusters. The electron redistribution [of type (1)] in a *free water molecule* in the molecular plane is shown in Fig. 1a, and perpendicular to this plane in Fig. 1b. In the condensed phase the water molecule is surrounded by several nearest neighbours. As a first approximation, the validity of which is discussed in more detail in the third section, the total electron rearrangement due to the first shell of neighbours is equal to the sum of the various neighbour-water pair contributions. It is thus informative to consider the nature of the constituent parts of the total redistribution.

The electron redistributions in the water dimer,[19,20] and in various water-cation[21–24] and water-anion[21,22] clusters have been calculated by many authors and at different levels of sophistication. From these studies, it is found that the electron redistribution in a water molecule due to a neighbouring cation or a hydrogen-bond donor on the oxygen side are qualitatively very similar. Likewise, the electron flow induced along the water O–H bond by an anion neighbour on the hydrogen side and by a hydrogen-bond acceptor are very similar, and moreover similar to the O–H electron deformation due to the cation neighbours. As a representative example, we will here discuss the electron rearrangement in a series of $Li^+ \cdot H_2O$ complexes, calculated with basis sets of double-zeta plus polarization quality. Only the lone-pair plane is displayed in Figs. 2 and 3.

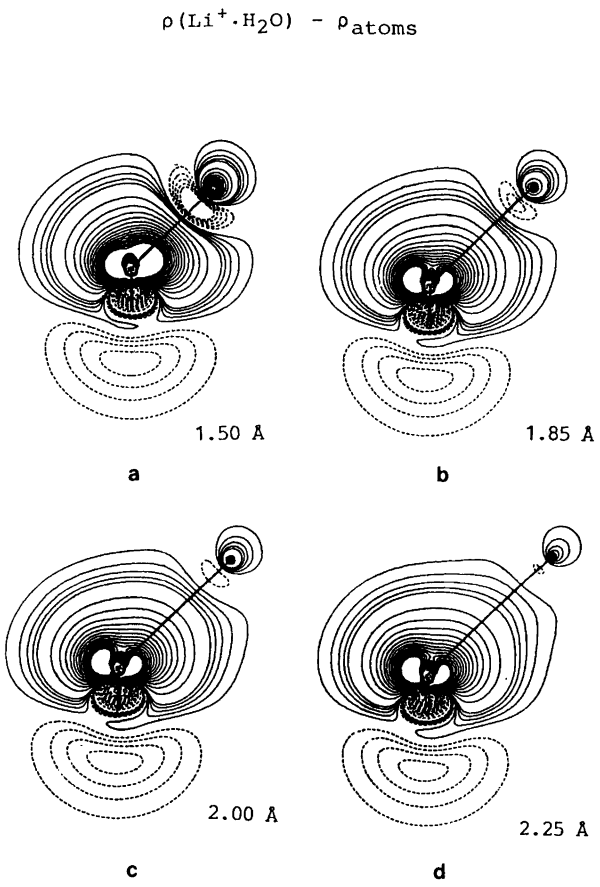

Fig. 2. Deformation electron density [of type (1)] for $Li^+ \cdot H_2O$ complexes with different cation–oxygen distances. The section shown bisects the H–O–H angle. Basis sets used were Dunning's[25] <4*s*2*p*/2*s*> contraction of Huzinaga's[17] (9*s*5*p*/4*s*) basis for O/H with polarization functions according to Roos and Siegbahn.[18] For Li^+ a <5*s*> contraction of Huzinaga's[17] (10*s*) basis augmented with a *p* function of exponent 0.525 was used. Contour levels at ±0.01, ±0.02,..., ±0.05, ±0.10,... e Å^{-3}.

The deformation densities in Fig. 2 are calculated with respect to atomic densities, and those in Fig. 3 with respect to the free molecules. The electron rearrangement for a water molecule interacting with a lithium ion can be summarized as follows:

(i) The major part of the deformation density in Fig. 2 is present already in the free water molecule (see Fig. 1b), and the intermolecular effects (Fig. 3) constitute relatively small perturbations of this density.

(ii) Two distinct features of intermolecular bonding can be noted in the lone-pair region for long and intermediate Li^+–O distances: the outer part of the electron density is pulled towards the lithium ion, while the opposite is true close to the oxygen atom.

(iii) For short Li^+–O distances, the reverse features appear compared to (ii). This is partly due to the increased exchange interaction, which removes electron density from the intermolecular region towards the bonding atoms (cf. Yamabe and Morokuma[22]).

(iv) The Li^+ ion induces a polarization in the water molecule with an electron migration along the O–H bond(s) leading to a substantial depletion of negative charge close to the hydrogen nuclei. This electron migration increases monotonically with decrease in the lithium–oxygen distance for the whole distance range covered in Figs. 2 and 3.

(v) The asymmetry in the outer parts of the lone-pair density caused by a lithium ion at a distance of 2.00 Å is only about 0.03 e Å^{-3} (see Figs. 2c

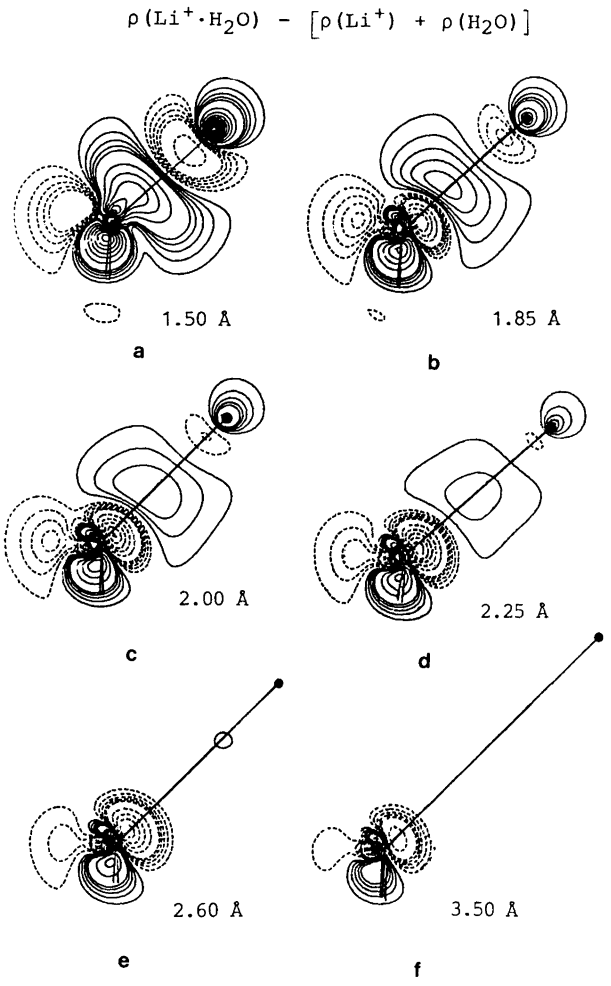

Fig. 3. Deformation electron density [of type (2)] for $Li^+ \cdot H_2O$ complexes with different cation–oxygen distances. The section shown bisects the H–O–H angle. Same basis sets and contour levels as in Fig. 2.

and 3c). A crystallographer may be tempted to regard this deformation feature as insignificant but, in doing so, is biased by the magnitude of the experimental uncertainty. Although difficult to detect experimentally, this bonding density represents a significant component of the intermolecular bonding. Close to the oxygen atom the induced asymmetry is much greater, but it occurs in a region which is virtually inaccessible to X-ray diffraction techniques.

(vi) Deformation density features close to the hydrogen atoms should be possible to detect in experimental X-ray studies. For a Li^+–O distance of 2.00 Å, the electron deficiency at the hydrogen nuclei is approximately -0.13 e Å^{-3} with respect to the free molecule (Fig. 3c, but in the molecular plane).

The crystalline environment. The deformation densities shown in Figs. 4a–b are calculated for an isolated cluster consisting of a water molecule surrounded by two lithium ions and two hydroxide ions in an approximately tetrahedral arrangement. The next-nearest neighbours and the crystal field counteract the electron redistribution caused by the nearest neighbours, and the magnitude of the corresponding redistribution is by no means negligible. When the crystalline environment of the $LiOH \cdot H_2O$ crystal[27] was simulated in an SCF calculation by point charges derived from a Mulliken population analysis, the defor-

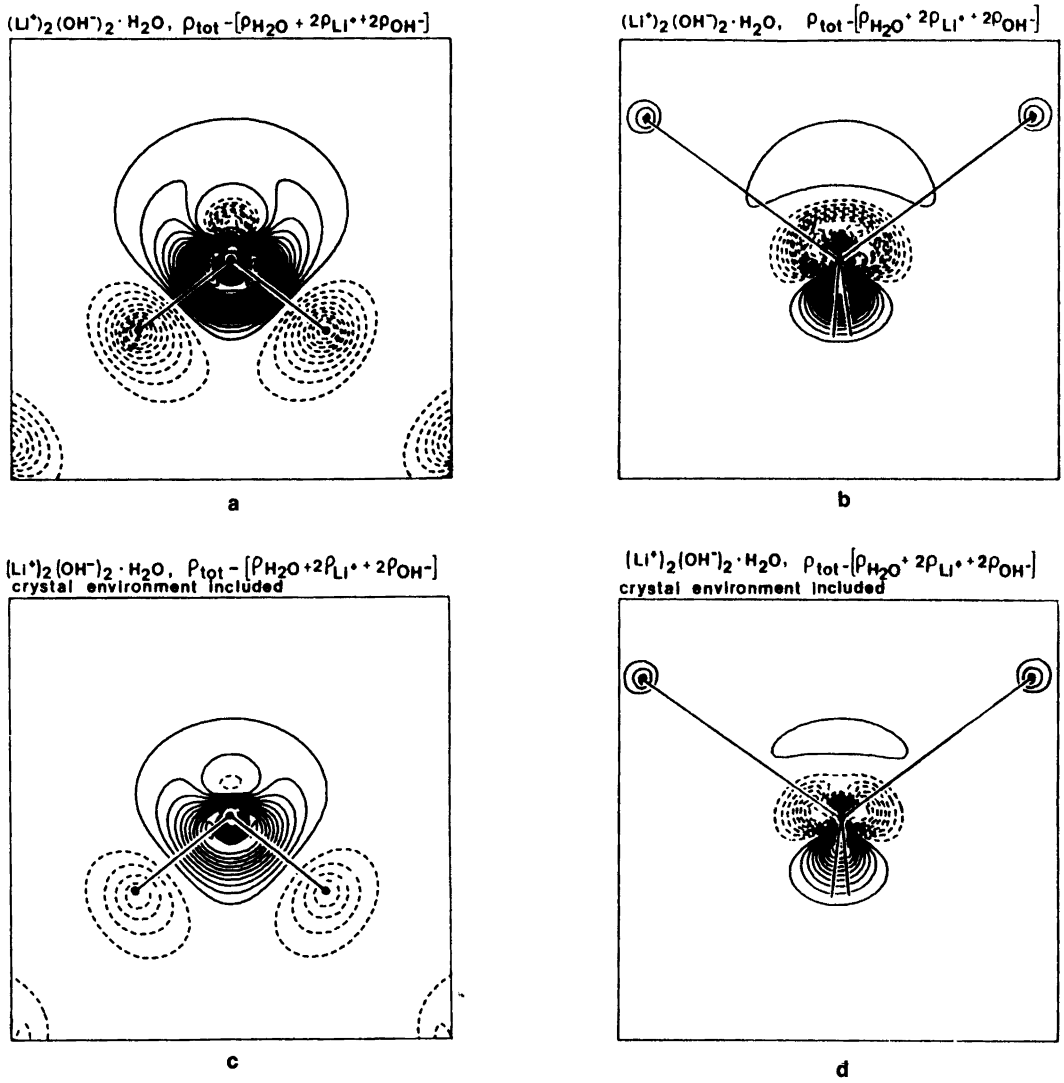

Fig. 4. Deformation electron density [of type (2)] for the $(Li^+)_2(OH^-)_2 \cdot H_2O$ complex in the $LiOH \cdot H_2O$ crystal, without (a–b) and with (c–d) the crystalline environment included in the calculation. For O and H the same basis sets were used as in Fig. 1. For Li^+ the (7*s*)/<3*s*> basis set of Clementi and Popkie,[26] augmented with a *p* function of exponent 0.525 (obtained by minimization of the energy of a $Li^+ \cdot H_2O$ complex) was used. Contour levels at ±0.05, ±0.10,... e Å^{-3}.

mation features decreased by about 50 % compared to the isolated complex (see Figs. 4c–d and Ref. 28). The agreement between the resulting theoretical maps and static experimental maps is then quite satisfactory, as shown in Fig. 5. We thus see that, in order to obtain quantitative agreement with experiment, the effect of the next-nearest neighbours and the rest of the crystal field has to be incorporated into the calculation.

Figs. 4c–d give an example of the electron redistribution due to intermolecular bonding in a hydrate where the water molecule is quite strongly bonded (O···O distances equal to 2.68 Å). Lunell (Ref. 30, Figs. 6b and 7b) gives another example, viz. for the more weakly bound wa-

Experimental

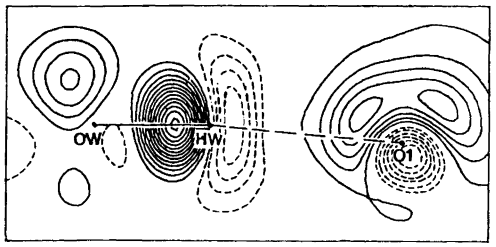

Theoretical

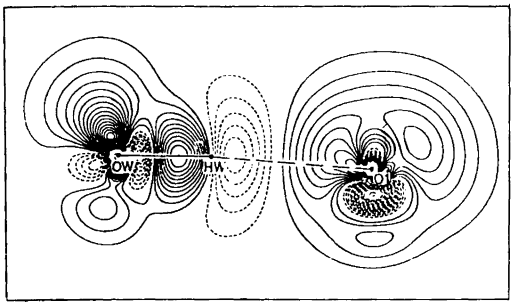

Fig. 5. Experimental and theoretical static deformation electron density [of type (1)] in the plane of the hydrogen bond in $LiOH \cdot H_2O$. The theoretical map is from Ref. 29, and the experimental from Ref. 27. Basis sets as in Fig. 1. Contour levels at ± 0.05, ± 0.10,... e Å^{-3}.

ter molecule in sodium hydrogen oxalate monohydrate (O···O distances equal to 2.80 Å). Here, the deformation density features due to the nearest neighbours and the crystalline environment are qualitatively the same as in lithium hydroxide monohydrate, but smaller: -0.12 and -0.17 e Å^{-3} at the hydrogen nuclei, -0.20 e Å^{-3} in the lone-pair region close to the oxygen atom, and $+0.02$ e Å^{-3} in the region between the cations and the oxygen atom. In experimental density maps, where the reference state consists of the atomic densities, the intermolecular deformation density effects are "superposed" on the intramolecular deformation. The fact that the latter is small in the region close to the hydrogen nuclei (see Fig. 1), combined with the fact that the intermolecular effects here are large (Fig. 4c) and the experimental accuracy is good leads one to conclude that the electron density at the hydrogen atoms should be a comparatively sensitive probe for intermolecular bonding effects in experimental maps. Since the water molecule is found to orient itself in a similar way with respect to surrounding positive and negative charges in most hydrates, these conclusions should be generally valid for crystalline hydrates.

Comparison with experiment. The observed electron density associated with a molecule in a crystal includes the smearing due to its vibrational motion. The deformation density peak heights (and troughs) in a "typical" hydrate at 300 K are reduced to approximately one third of their static values. Moreover, the crystal structure has a direct influence on the vibrational motion of the bound molecules, and differences in the vibrational scheme from one structure to another will introduce differences which are not directly related to the static deformation densities discussed above. These points should be borne in mind when analyzing experimental dynamic densities for intermolecular effects.

Dynamic experimental deformation density maps for a series of hydrogen bonds with O···O distances ranging from 2.45 to 2.80 Å are shown in Fig. 6. These are all 120 K studies, except for $LiOH \cdot H_2O$, where the tightly bound structure renders the room-temperature thermal parameters unusually small. The maximum peak heights for the O–H bonds are all approximately 0.30 e Å^{-3}, and the density at the hydrogen positions less than 0.10 e Å^{-3}, verifying the quality of the experimental results. The deformation density at the hydrogen positions follows nicely the trend predicted by the theoretical calculations, namely that intermolecular effects should show up as a larger electron density depletion the stronger the hydrogen bond. It should also be added here that the shorter the O···O bond, the more the O–H bond is stretched, with an accompanying electron depletion (see Figs. 2g–h in Ref. 9) which reinforces the intermolecular trend.

Fig. 7 is a compilation of experimental X–N electron density studies of hydrates reported up until 1975.[33] The maps show a variation which is much larger than can reasonably be expected to arise from the influence of different bonding environments or differences in thermal motion. Unfortunately, the majority of these deformation maps, although representing pioneering and extremely valuable work, display physically quite unrealistic features and it must be concluded that the densities for these water molecules are sub-

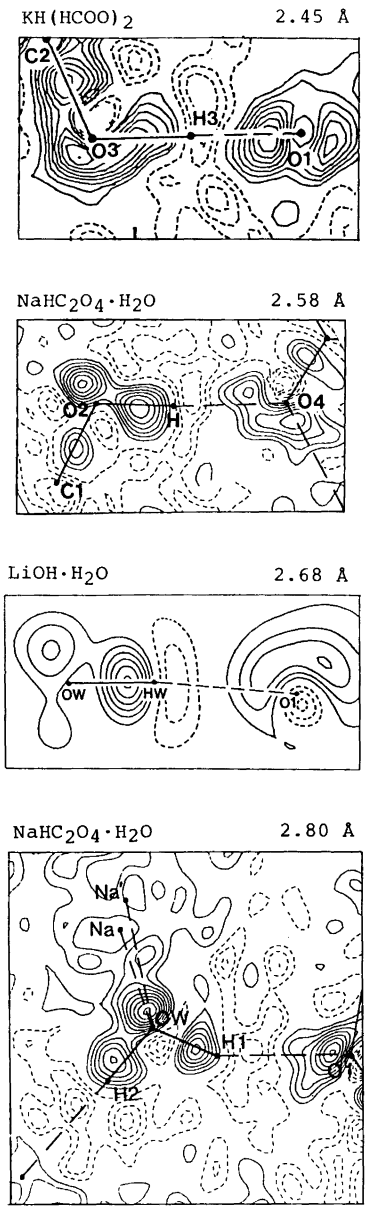

Fig. 6. Experimental dynamic deformation density maps for O–H···O hydrogen bonds of different lengths. The $KH(HCOO)_2$ (Ref. 31) and $NaHC_2O_4 \cdot H_2O$ (Ref. 32) densities are from X–N studies at 120 K, while the $LiOH \cdot H_2O$ (295 K) density (Ref. 27) is derived from a deformation refinement using multipolar functions according to Hirshfeld.[12] Contour levels at ±0.05, ±0.10,... e Å^{-3}.

ject to large errors. A similar compilation including more recent work was made in 1984;[39] an excerpt of this is given in Fig. 8, and shows that the experimental accuracy had by then improved considerably. This is due in part to the availability of better-quality neutron diffraction data, low-temperature data and new refinement procedures. The experimental noise in Fig. 8 is low and the peak heights are of the expected order of magnitude. However, inspection of the water molecules reveals no clear-cut trends in the variation of the deformation density features with structural environment. It should then be borne in mind that the O··O hydrogen-bond lengths for the different structures in Fig. 8 vary between 2.68 and 2.85 Å, and that the static deformation density is expected to vary by less than 0.10 e Å^{-3} in this hydrogen-bond range (cf. Fig. 4 of Ref. 9) and the dynamic density even less. In view of the fact that the experimental accuracy is generally not better than 0.05 e Å^{-3}, it must be concluded that these intermolecular effects are at the limit of what experiment can measure today.

Intermolecular energies and electron density distributions

In "molecular modelling" it is usual to focus on the intra- and/or intermolecular energies rather than the electron densities themselves. In Molecular Dynamics studies, for example, the intermolecular forces determine the molecular "trajectories", and the key part of an MD simulation code is usually an energy-force double loop of the form

```
    DO 100 I = 1, NMOL-1
    DO 100 J = I+1, NMOL
    E(I,J) = some simplified expression
    F(I,J) = another simplified expression
100 CONTINUE                                    (3)
```

where NMOL is the number of molecules in the MD system. This piece of code involves two important simplifications, both of which are imposed by CPU time restrictions. The first involves the *functional form* of the energy and force expressions themselves. The second is the assumption that the interaction within the system can be expressed in terms of *pair energies,* and that non-additive effects are negligible. This is not strictly true for any real system, but it is often

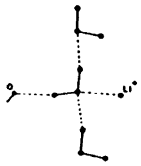

$LiHCOO \cdot H_2O$
(Ref. 34)

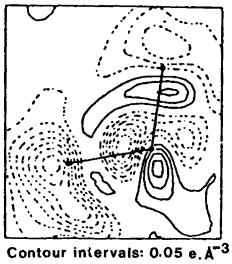

Contour intervals: 0.05 e.Å^{-3}

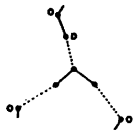

α- $(COOD)_2 \cdot 2D_2O$
(Ref. 37)

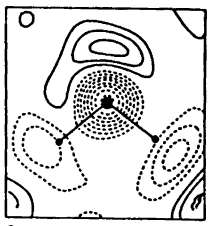

Contour intervals: 0.05 e.Å^{-3}

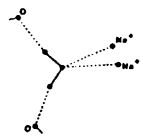

$NaHC_2O_4 \cdot H_2O$
(Ref. 35)

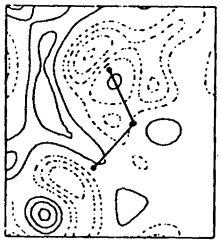

Contour intervals: 0.025 e.Å^{-3}

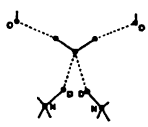

$(ND_4)_2C_2O_4 \cdot D_2O$
(Ref. 38)

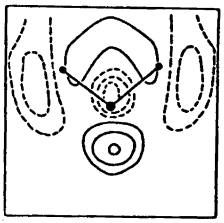

Contour intervals: 0.05 e.Å^{-3}

$NaClO_4 \cdot H_2O$
(Ref. 36)

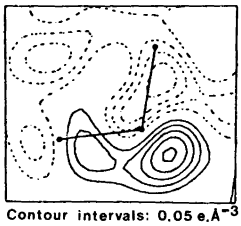

Contour intervals: 0.05 e.Å^{-3}

Fig. 7. Experimental X–N deformation density maps of hydrates studied prior to 1975. References and contour intervals are given in the figure.

the only feasible way of performing a simulation experiment within a sufficiently short CPU time (some simulation studies including many-body interactions do exist; see, for example, Refs. 43–48).

One approach to obtaining analytical potentials for use in molecular modelling and simulation applications is to fit *ab initio* calculated energies for a large number of molecular arrangements to simple analytical potential expressions. However, SCF calculations and electron density distributions can be of value in the construction of potentials, even when empirical or effective pair potentials are used. The multipolar moments of the calculated electron density can, for example, serve as guide-lines in the construction of reasonable molecular pair potentials by providing parameters for the electrostatic part of these potentials. Various schemes have been designed for the derivation of charges from the wavefunctions or the electron distribution; those of Mulliken,[49] Bader[50] and Hirshfeld[51] are but a few.

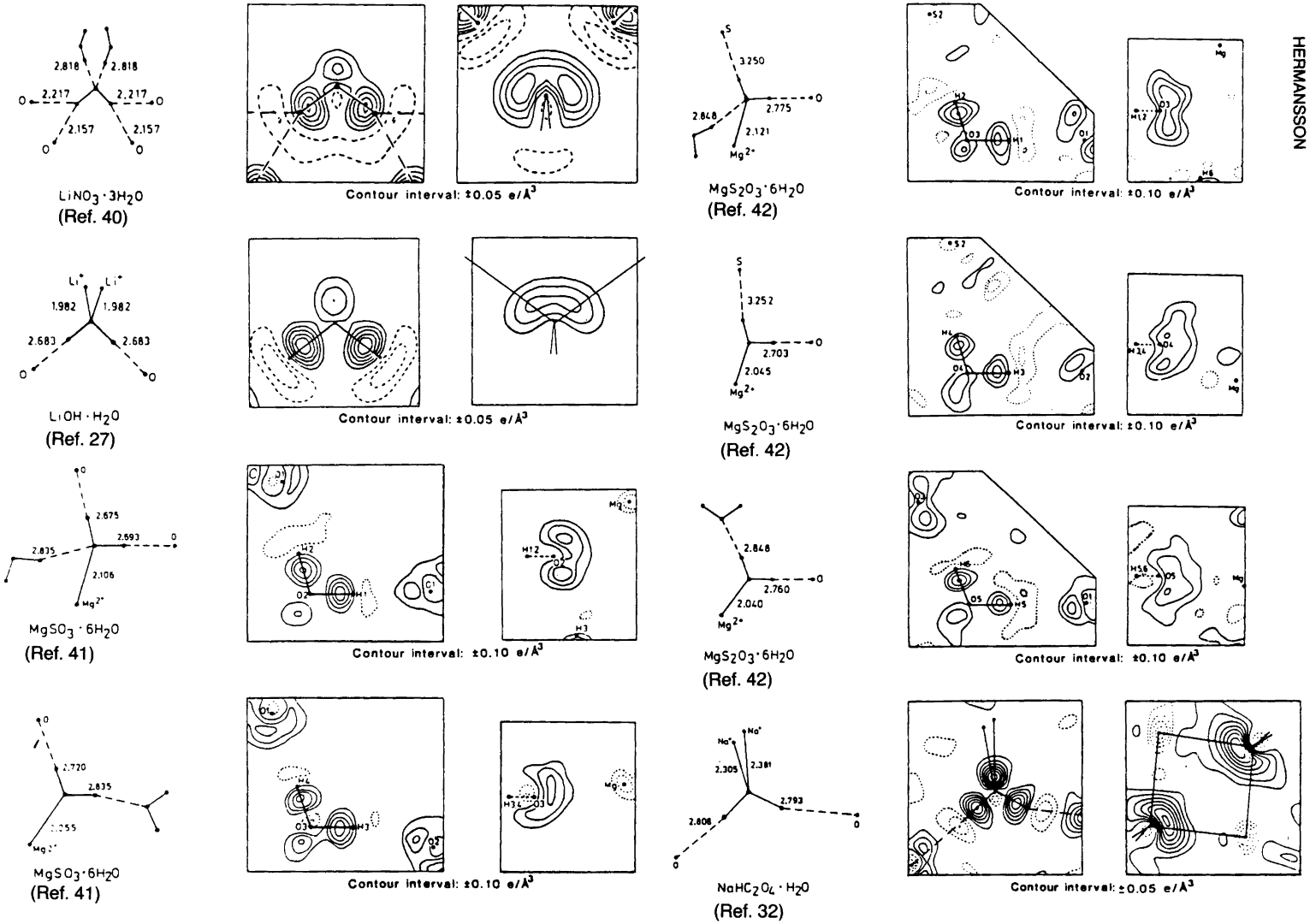

Fig. 8. A selection of experimental, dynamic deformation density maps for hydrates studied after 1980 (see text). References and contour intervals are given in the figure.

The concept of pair-additivity also greatly profits from a combined description in terms of energy and electron distribution. Following Hankins, Moskowitz and Stillinger,[52] the 3-body (non-additive) contribution to the interaction energy of a molecular triplet (*ijk*) is defined as the difference between the total interaction energy and the sum of the pair interaction energies, i.e.:

$$\Delta^3E(ijk) = \Delta E(ijk) - [\Delta E(ij) + \Delta E(ik) + \Delta E(jk)] \quad (4)$$

where

$$\Delta E(ij) = E(ij) - [E(i) + E(j)] \quad (5)$$

and

$$\Delta E(ijk) = E(ijk) - [E(i) + E(j) + E(k)]. \quad (6)$$

The definition of 2-body and 3-body contributions to the deformation density is completely analogous.

Several *ab initio studies* on water triplets (see, for example, Refs. 52–55) have shown the 3-body energy to be up to 10–15 % of the total interaction energy for certain triplets. For ion-water complexes, the 3-body interaction is generally larger (cf. Refs. 52–62). Calculations on Al^{3+} and Mg^{2+} hexaaqua complexes have shown the non-additive contribution to the interaction energy to be as large as 30 % in the former case and 20 % in the latter.[62]

With the help of the fictitious $\oplus \cdot (H_2O)_2$ complex in Fig. 9 we will discuss here the origin of the 3-body non-additive effects on energies and electron density distributions. Based on previous investigations[9] of the sensitivity of the deformation density of a water molecule to the position of a positive point charge, the geometry of the $\oplus \cdot (H_2O)_2$ complex in Fig. 9 was chosen so as to maximize the effects of non-additivity. *If* the electron redistributions in Fig. 9 are additive, eqn. (4) (as applied to the electron densities) gives:

$$\text{Fig. 9d} = \text{Fig. 9a} + \text{Fig. 9b} + \text{Fig. 9c}. \quad (8)$$

Inspection of Fig. 9 shows that, to a good approximation, this is indeed true. This is also reflected in the charges derived from the Mulliken population analysis. The charges on O(1)/H(1)/H(2) are −0.52/+0.26/+0.26 for the free $H_2O(1)$ molecule, −0.66/+0.39/+0.27 in Fig. 9a, −0.57/+0.31/+0.24 in Fig. 9c, and −0.71/+0.41/+0.26 in the $\oplus \cdot (H_2O)_2$ complex in Fig. 9d. One can thus see that the *charge shift* for O(1), for example, due to the point charge, is the same irrespective of whether $H_2O(1)$ is bonded to $H_2O(2)$ or not, which is another way of expressing the additivity of the Mulliken charge shifts.

In contrast, the intermolecular interaction *energies* show a significant component of non-additivity. The interaction energies for the different "sub-complexes" are given in Fig. 9. The total interaction energy for the whole complex is −171 kJ mol^{-1}, while the three 2-body contributions, −102, −23 and −18 kJ mol^{-1}, sum to −143 kJ mol^{-1}. The 3-body correction to the energy is thus −28 kJ mol^{-1}. This effect of cooperativity can be seen as the result of the interaction of, for example, the $H_2O(1)$ molecule with the $\oplus$ charge, which increases the polarity of the molecule and makes it a more efficient hydrogen-bond donor to $H_2O(2)$.

An investigation of 2-, 3-, 4- and 5-body effects on electron density and energies in a tetrahedral $(H_2O)_5$ and two $\oplus_2\ominus_2 \cdot H_2O$ complexes has been carried out.[63] Here, it was also found that many-body effects on the deformation electron density are indeed very small and that it is mainly the additive parts of the electron redistribution which give rise to non-additive effects in the energy.

These model calculations on different crystal-like fragments constitute a tool for evaluating the importance of many-body effects on different properties. Their final effect on thermodynamic quantities the overall structural and dynamic properties in a real many-body system should be evaluated by computer simulation techniques.

Conclusions

Over the years there has been steady progress in the derivation of reliable positional and thermal parameters and electron distributions from diffraction data. This is a result of technical advances involving the development of reliable crystal cooling devices and readier access to thermal neutron reactors, as well as of advances in methodology, such as better correction procedures for extinction and thermal diffuse scattering, and access to multipolar refinement techniques.

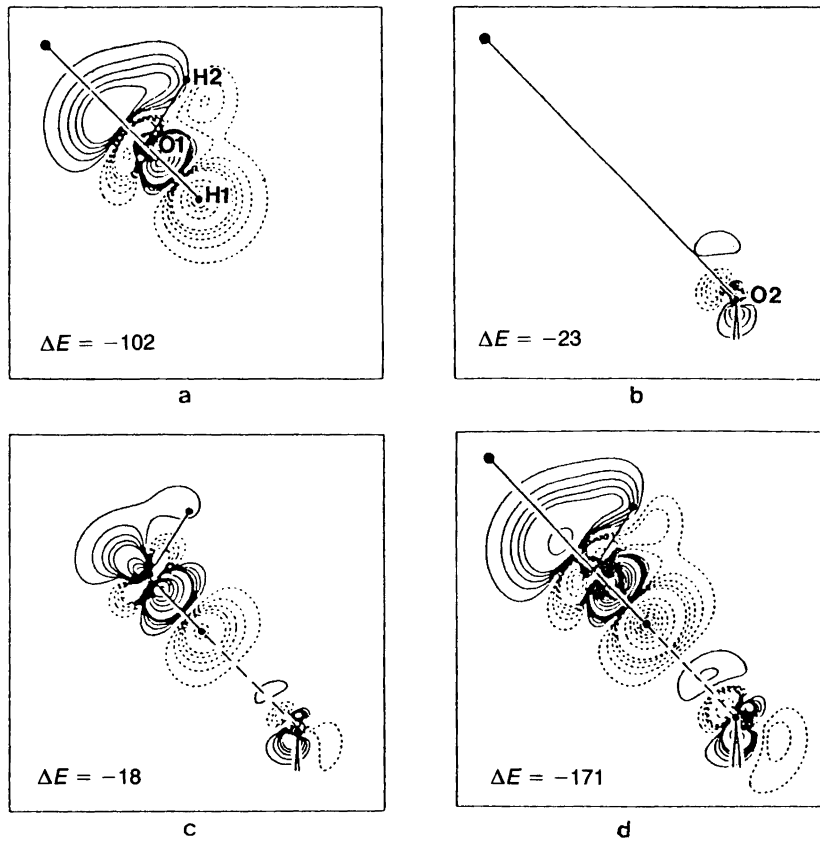

Fig. 9. Additivity of theoretical interaction energies and static deformation densities [of type (2)] for a $\oplus \cdot H_2O \cdot H_2O$ complex. The point charge–O(1) distances is 2.00 Å, and the O(1)···O(2) distance 2.75 Å. Basis sets are the same as in Fig. 2. Contour levels at ±0.01, ±0.02,... ±0.05, ±0.10,... e Å^{-3}. Energies in kJ mol^{-1}.
(a) $f[\oplus \cdot H_2O(1)] - f[H_2O(1)]$, where $f = \varrho(r)$ or $f = E$. (b) $f[\oplus \cdot H_2O(2)] - f[H_2O(2)]$, where $f = \varrho(r)$ or $f = E$.
(c) $f[H_2O(1) \cdot H_2O(2)] - f[H_2O(1)] - f[H_2O(2)]$, where $f = \varrho(r)$ or $f = E$.
(d) $f[\oplus \cdot H_2O(1) \cdot H_2O(2)] - f[H_2O(1)] - f[H_2O(2)]$, where $f = \varrho(r)$ or $f = E$.

Parallel to improvements in the experiments, there has been an enormous development in theoretical work. Quantum-mechanical and statistical-mechanical methods have improved thanks to new theory, new algorithms and, not least, the availability of faster computers. In many areas of physics and chemistry, joint experimental and computational studies constitute a powerful approach which serves as a check on the reliability of both methods. More importantly, model computations can provide new insights and new quantities not directly obtainable from the experimental data. Examples of such information have been discussed in this review from the point of view of a crystallographer. We conclude that:

(i) The agreement between high-quality experimental and theoretical electron density maps is generally good. Both approaches have, however, their own, very different limitations; neither can be clearly favoured at present. In order to observe reliable intermolecular bonding features in experimental electron densities, an increase in the overall precision of the experimental data is needed. At the same time, it is hoped that computer evolution will soon permit the routine use

of very large basis sets in *ab initio* calculations of sizeable clusters, and reliable correction for correlation effects in energies and densities for such systems.

(ii) Quantum-mechanical calculations on well-designed model systems are able to give the qualitative features and the magnitude of the electron rearrangement due to inter- and intramolecular bonding in a crystalline hydrate.

(iii) The effects of *inter*molecular bonding in crystalline hydrates are often at the limit of what can be measured experimentally today.

(iv) For molecular crystals containing ions or polar molecules, the effects of next-nearest neighbours and crystal field on the molecular electron redistribution are found to be large and must therefore be included in the theoretical calculations.

(iv) Theoretical calculations allow the study of the influence of different components in the environment separately. One application is the study of non-additivity in intermolecular interactions. Three-body effects give an appreciable contribution to the interaction energies for water and water-ion clusters, but are very small for the electron rearrangement.

(vi) A *combined* discussion of the experimental structure and electron distributions on the one hand, and intermolecular bond energies (from quantum-mechanical calculations or molecular modelling computations) on the other, brings much insight into a structural analysis.

(vii) Molecular Dynamics simulation is a powerful method for learning about dynamical processes in crystals. With access to faster computers it will be possible to use more elaborate interaction models, and increase the size of the simulation systems and the real time-span covered by the simulation runs, a development which will make theoretical results more and more realistic and open up new fields of research.

References

1. Righini, R. *Physica B 131* (1985) 234.
2. Rees, B. *Isr. J. Chem. 16* (1977) 154; *Ibid.* 180.
3. Feil, D. *Isr. J. Chem. 16* (1977) 149.
4. Wojcik, M. C. and Hermansson, K. *Acta Chem. Scand., Ser. A 41* (1987). 562.
5. Pullman, B. *Interatomic Interactions: From Diatomics to Biopolymers,* Wiley, New York 1978.
6. Raznakievich, H. and Orville-Thomas, W. J. *Molecular Interactions,* Wiley, New York 1980, Vols, 1, 2 and 3.
7. Hirshfeld, F. L., Guest Ed., *Isr. J. Chem. 16* (1977).
8. Coppens, P. and Hall, M. B. *Electron Distributions and the Chemical Bond,* Plenum, New York 1977.
9. Hermansson, K. *Acta Crystallogr., Sect. B 41* (1985) 161.
10. Coppens, P. *Acta Crystallogr., Sect. B 30* (1974) 255.
11. Stewart, R. F. *J. Chem. Phys. 51* (1969) 4569.
12. Hirshfeld, F. L. *Acta Crystallogr., Sect. B 27* (1971) 769.
13. Breitenstein, M., Dannöhl, H., Meyer, H., Schweig, A. and Zittlau, W. In: Coppens, P. and Hall, M. B., Eds., *Electron Distributions and the Chemical Bond,* Plenum, New York 1977.
14. Smith, V. H., Jr. *Phys. Scr. 15* (1977) 147.
15. Feil, D. *Chem. Scr. 26* (1986) 395.
16. Dunning, T. H., Jr. *J. Chem. Phys. 55* (1971) 716.
17. Huzinaga, S. *J. Chem. Phys. 42* (1965) 1293.
18. Roos, B. and Siegbahn, P. *Theor. Chim. Acta 17* (1970) 199.
19. Yamabe, S. and Morokuma, K. *J. Am. Chem. Soc. 97* (1975) 4458.
20. Diercksen, G. H. F. *Theor. Chim. Acta 21* (1971) 335.
21. Schuster, P., Jakubetz, W. and Marius, W. *Topics Curr. Chem.* Springer-Verlag, Berlin 1975, Vol. 60, p. 1.
22. Diercksen, G. H. F. and Kraemer, W. P. *Munich Reference Manual,* Special Techn. Report, Max Planck Institut für Physik und Astrophysik, Munich 1981.
23. Demoulin, D. and Pullman, A. *Theor. Chim. Acta 49* (1978) 161.
24. Hermansson, K., Olovsson, I. and Lunell, S. *Theor. Chim. Acta 64* (1984) 265.
25. Duning, T. H., Jr. *J. Chem. Phys. 53* (1970) 2823.
26. Clementi, E. and Popkie, H. *J. Chem. Phys. 57* (1972) 1077.
27. Hermansson, K. and Thomas, J. O. *Acta Crystallogr., Sect. B 38* (1982) 2555.
28. Hermansson, K. and Lunell, S. *Chem. Phys. Lett. 80* (1981) 64.
29. Hermansson, K. and Lunell, S. *Acta Crystallogr., Sect. B 38* (1982) 2563.
30. Lunell, S. *J. Chem. Phys. 80* (1984) 6185.
31. Hermansson, K. and Tellgren, R. *To be published.*
32. Delaplane, R. G., Tellgren, R. and Olovsson, I. *Acta Crystallogr., Sect. B 44. Submitted for publication.*

33. Thomas, J. O. *Presented at the II European Crystallographic Meeting*, Keszthely, Hungary 1974.
34. Thomas, J. O., Tellgren, R. and Almlöf, J. *Acta Crystallogr., Sect. B 31* (1975) 1946.
35. Tellgren, R. and Thomas, J. O. *Private communication* (1975).
36. Berglund, B., Tellgren, R. and Thomas, J. O. *Acta Crystallogr., Sect. B 32* (1976) 2444.
37. Coppens, P., Sabine, T. M., Delaplane, R. G. and Ibers, J. A. *Acta Crystallogr., Sect. B 25* (1969) 2451.
38. Taylor, J. C. and Sabine, T. M. *Acta Crystallogr., Sect. B 28* (1972) 3340.
39. Hermansson, K. *Acta Universitatis Upsaliensis* (Abstracts of Uppsala University Dissertations from the Faculty of Science) *744* (1984).
40. Hermansson, K., Thomas, J. O. and Olovsson, I. *Acta Crystallogr., Sect. C 40* (1984) 335.
41. Bats, J. W., Fuess, H. and Elerman, Y. *Acta Crystallogr., Sect. B 42* (1986) 552.
42. Elerman, Y., Bats, J. W. and Fuess, H. *Acta Crystallogr., Sect. C 39* (1983) 515.
43. Barnes, P., Finney, J. L., Nicholas, J. D. and Quinn, J. E. *Nature (London) 282* (1979) 459.
44. Gellatly, B. J., Quinn, J. E., Barnes, P. and Finney, J. L. *Mol. Phys. 59* (1983) 949.
45. Clementi, E. and Corongiu, G. *Int. J. Quantum Chem.: Quantum Biology Symposium 10* (1983) 31.
46. Detrich, J., Corongiu, G. and Clementi, E. *Int. J. Quantum Chem.: Quantum Chemistry Symposium 18* (1984) 701.
47. Lybrand, T. P. and Kollman, P. A. *J. Chem. Phys. 83* (1985) 2923.
48. Wojcik, M. C. and Clementi, E. *J. Chem. Phys. 85* (1986) 6085.
49. Mulliken, R. S. *J. Chem. Phys. 23* (1955) 1833.
50. Bader, R. F. W. and Nguyen-Dang, T. T. *Adv. Quantum Chem. 14* (1981) 63.
51. Hirshfeld, F. L. *Isr. J. Chem. 16* (1977) 198.
52. Hankins, D., Moskowitz, J. W. and Stillinger, F. H. *J. Chem. Phys. 53* (1970) 4544; *Ibid. 59* (1973) 995.
53. Clementi, E., Kolos, W., Lie, G. C. and Ranghino, G. *Int. J. Quantum Chem. 17* (1980) 377.
54. Yoon, B. J., Morokuma, K. and Davidson, E. R. *J. Chem. Phys. 83* (1985) 1223.
55. Kim, K. S., Dupuis, M., Lie, G. C. and Clementi, E. *Chem. Phys. Lett. 131* (1986) 451.
56. Kollman, P. A. and Kuntz, I. D. *J. Am. Chem. Soc. 94* (1972) 9236; *Ibid. 96* (1974) 766.
57. Kistenmacher, H., Popkie, H. and Clementi, E. *J. Chem. Phys. 61* (1974) 799.
58. Kress, J. W., Clementi, E., Kozak, J. J. and Schwarz, M. E. *J. Chem. Phys. 63* (1975) 3907.
59. Clementi, E., Kistenmacher, H., Kolos, W. and Romano, S. *Theor. Chim. Acta 55* (1980) 257.
60. Perez, P., Lie, W. K. and Prohofsky, E. W. *J. Chem. Phys. 79* (1983) 388.
61. Mathers, T. L. and Kestner, N. R. *Int. J. Quantum Chem.: Quantum Chem. Symposium 19* (1986) 297.
62. Probst, M. M. *Chem. Phys. Lett. 137* (1987) 229.
63. Hermansson, K. *To be published.*

Received September 4, 1987.